

Supporting Information

for

Rational Design of Supramolecular Hemin/Q-Quadruplex-Dopamine Aptamer Nucleoapzyme Systems with Superior Catalytic Performance

by

H. Bauke Albada, Eyal Golub and Itamar Willner

<u>Table Of Contents</u>	<u>page</u>
Oxidation of ABTS²⁻ to ABTS⁻ by nucleoapzyme structures 3t–9t	2
Melting curves of supramolecular nucleoapzymes 6t and 6r	2
Computational simulations of the 5r and 6r systems	3
Computational simulations of the 7t, 8t, and 9t systems.....	3
Saturation kinetics curves for the three different states in the switchable system	4
CD spectroscopic analysis of the switching event from 4tx/7 + 6 to 4tx/6 + 7/8.....	5

Oxidation of ABTS^{2-} to $\text{ABTS}^{\bullet-}$ by nucleoapzyme structures **3t–9t**

The oxidation of ABTS^{2-} to its radical anion $\text{ABTS}^{\bullet-}$ was performed in a microtiterplate (BioTek Hybrid H1 platereader). Kinetics of the oxidation reactions were followed by monitoring the appearance of the radical anion ($\text{ABTS}^{\bullet-}$) at 414 nm over a time-period of 10 min. Reactions were initiated by the addition of H_2O_2 (100 μM) to the ABTS^{2-} (50 μM) solution in the presence of the various nucleoapzyme systems. The measurements were performed in duplicate.

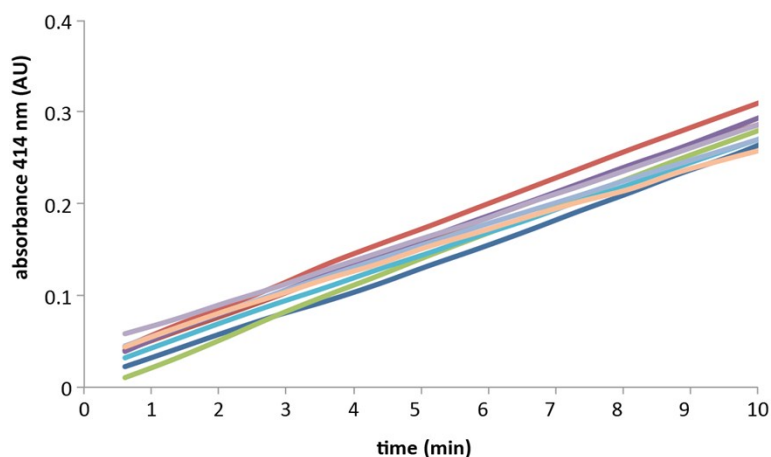


Figure S1. Time-dependent increase in the absorbance of $\text{ABTS}^{\bullet-}$ as a result of the supramolecular nucleoapzyme-catalysed H_2O_2 -mediated oxidation of ABTS^{2-} .

Melting curves of supramolecular nucleoapzymes **6t** and **6r**

Thermal denaturation profiles for **6t** and **6r** were measured using 1 μM DNA in 50 mM MES buffer (pH = 5.5, 200 mM KCl, 2 mM MgCl_2). The temperature was raised with 1 $^\circ\text{C}/\text{min}$. For both systems, two melting points were observed: $T_{m,1}$ 43 $^\circ\text{C}$ (for **6t** and **6r**), and $T_{m,2}$ = 60 $^\circ\text{C}$ (for **6r**) and $T_{m,2}$ = 64 $^\circ\text{C}$ (for **6t**). The first melting point is assigned to the dissociation of the small hairpins in the DBA unit, the second melting point is assigned to the dissociation of the larger double-strand DNA unit that is applied to merge the GQ unit and the DBA unit L/L'. The presence of the five triplex-forming bases in **6t** stabilize this interaction, when compared to the non-stabilized system **6r**, leading to the higher observed melting point.

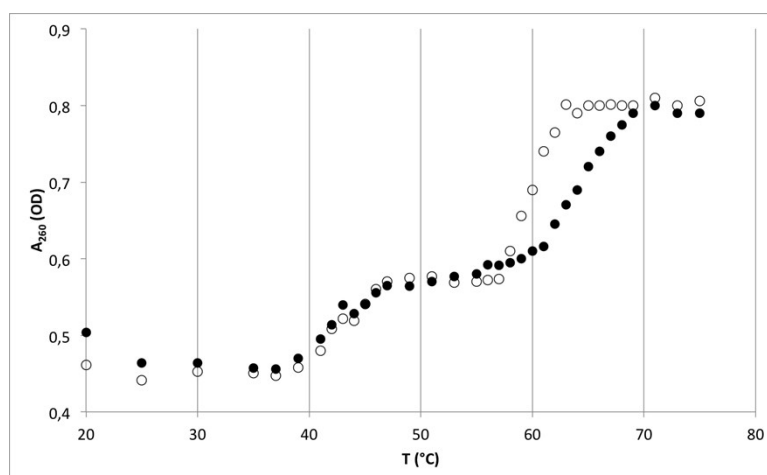


Figure S2. UV melting profile of **6t** (solid circles) and **6r** (open circles) at 260 nm in 50 mM MES, pH = 5.5, 200 mM KCl, 2 mM MgCl_2 . Concentration DNA = 1 μM .

Computational simulations of the **5r** and **6r** systems

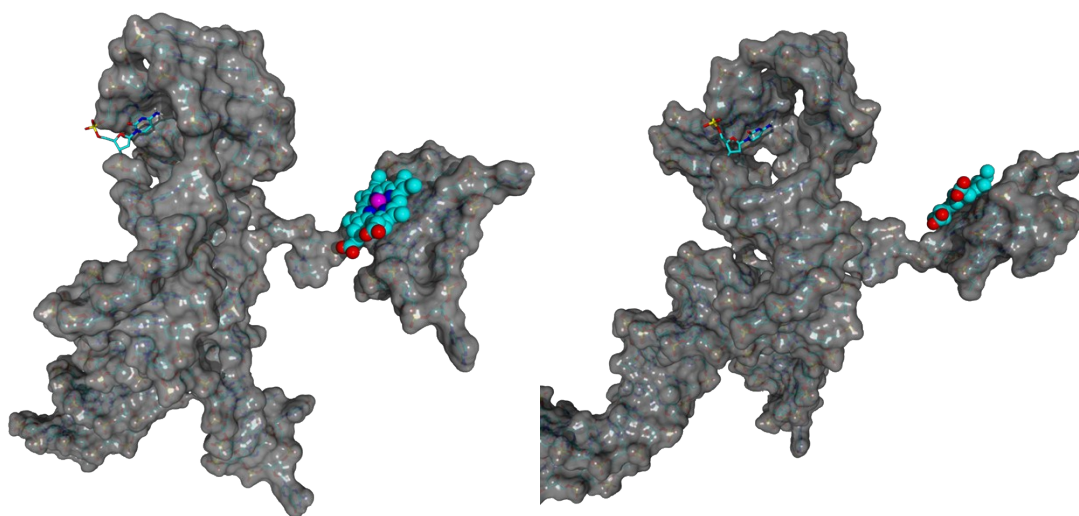
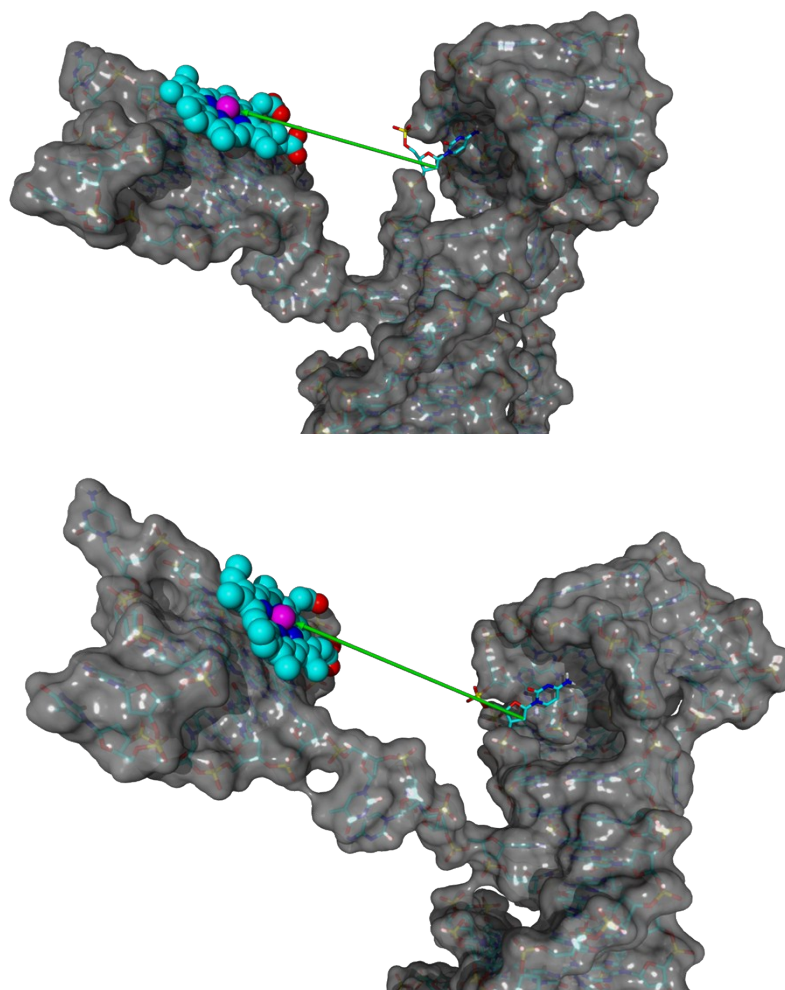


Figure S3. Models of non-stabilized supramolecular system systems **5r** (*left*) and **6r** (*right*).

Computational simulations of the **7t**, **8t**, and **9t** systems



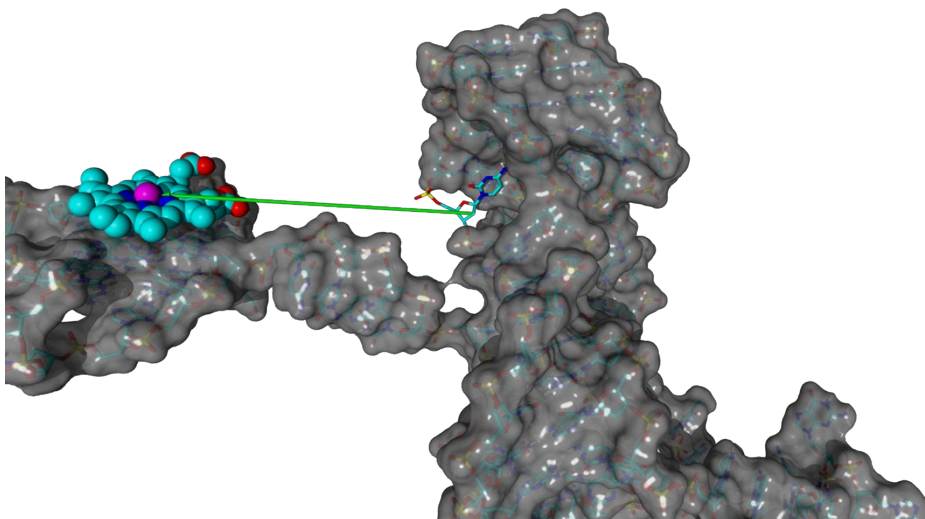


Figure S4. Models of triplex-stabilized supramolecular system systems **7t** (*top*), **8t** (*middle*), and **9t** (*bottom*). Lengths of the arrows are: 25 Å, 29 Å, and 33 Å, for **7t**, **8t**, and **9t**, respectively.

Saturation kinetics curves for the three different states in the switchable system

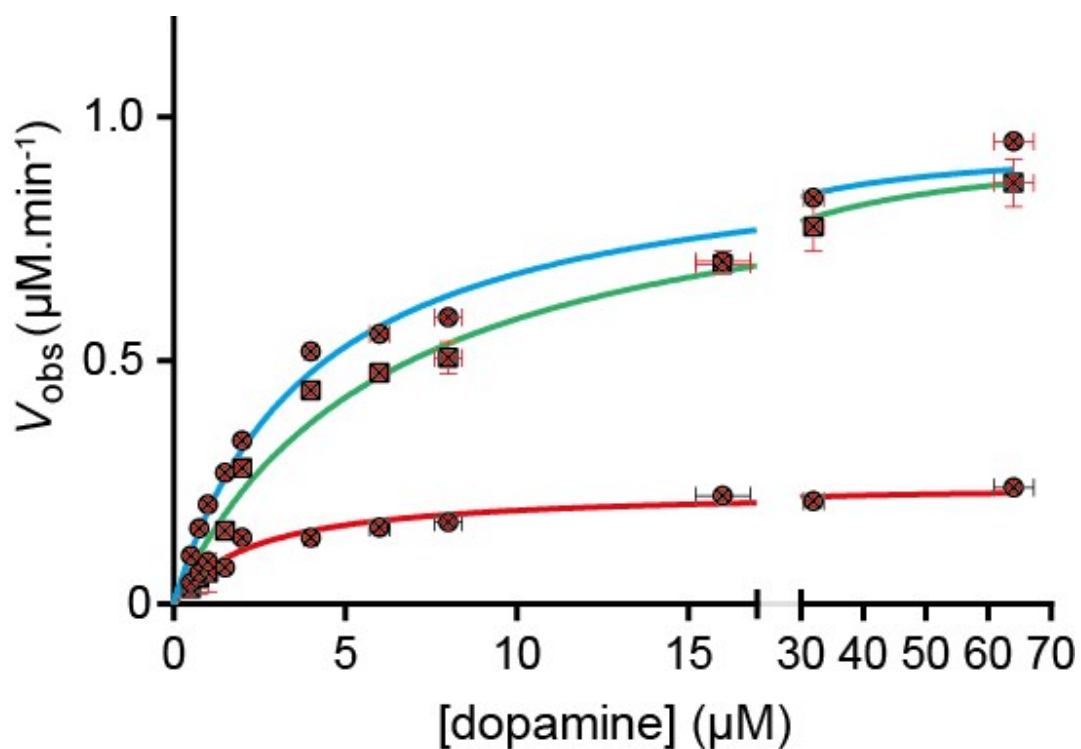


Figure S5. Kinetics curves of the switchable supramolecular nucleopzyme system **4tx/6** (*blue*), separated entities **4tx/7** and **6** (*red*), and system **4tx/6** in the presence of duplex **7/8** (*green*).

Tables S1. Kinetic parameters of the various supramolecular nucleopzyme structures with respect to the oxidation of dopamine (**1**) to aminochrome (**2**) in the presence of H₂O₂.

System	k_{cat} (10^{-3} s^{-1}) ^a	K_{M} (μM)	V_{max} ($\mu\text{M}\cdot\text{min}^{-1}$)	k_{cat}/k_2^b
4tx/6	21.3 ± 0.5	4.0 ± 0.3	0.95 ± 0.02	23.7
4tx/7	5.3 ± 0.2	2.3 ± 0.3	0.24 ± 0.01	5.9
4tx/6 + 7/8	21.2 ± 0.7	6.2 ± 0.7	0.95 ± 0.03	23.6

Conditions: 0.5–64 μM dopamine, 100 μM H₂O₂; 0.74 μM active catalyst; buffer: 50 mM MES, pH = 5.5, 200 mM KCl, 2 mM MgCl₂. *Notes:* ^a $k_{\text{cat}} = V_{\text{max}} / [\text{catalyst}] = V_{\text{max}} / 0.74$. ^b the rate constant for the hGQ DNAzyme (**1**) is: $k_2 = (0.9 \pm 0.1) \cdot 10^{-3} \text{ s}^{-1}$.

We note that for the system **4tx/6** and **4tx/6 + 7/8** the K_{M} values differ by ca. 50% while all other kinetic parameters are similar (k_{cat} , V_{max}). This apparent difference in the K_{M} values is attributed to the fact that dopamine reveals non-specific affinity towards duplex DNA (in this case dsDNA **7/8**). Since K_{M} values are predominantly determined by the rates (v) at relatively low concentrations of dopamine, this non-specific binding of dopamine in the **4tx/6 + 7/8** mixture leads to a lower substrate concentration for the nucleopzyme at these lower concentrations, and thus to a higher K_{M} value. This fact is, also, reflected by the lower V_{obs} values for the **4tx/6 + 7/8** system when compared to the **4tx/6** system alone, specifically at the lower dopamine concentration regiment (at $\leq 8 \mu\text{M}$ dopamine). At high concentrations of dopamine (at $\geq 16 \mu\text{M}$ dopamine), at which the V_{max} -values are calculated, this side-effect binding is negligible, leading to similar V_{max} values of the two systems.

CD spectroscopic analysis of the switching event from **4tx/7 + 6** to **4tx/6 + 7/8**

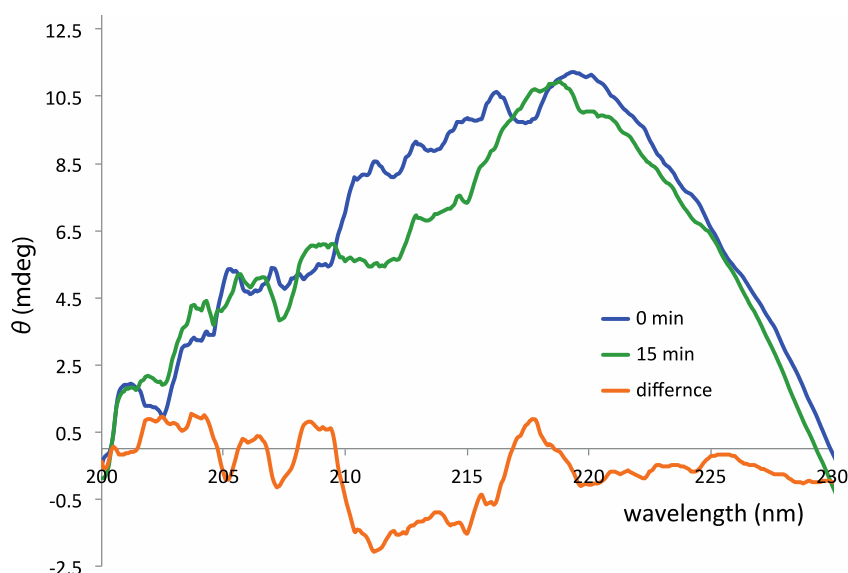


Figure S6. CD spectra of **4tx/6 + 7/8** obtained 0 and 15 min after addition of “ON” switch (**8**) to the mixture of **4tx/7 + 6**. Appearance of the negative feature around 213 nm shows the time-dependent formation of the triplex feature.